Heavy flavour production and decay in ATLAS

Adam Barton
On Behalf of the ATLAS collaboration

Introduction

- Flavor Physics at ATLAS
  - Measurements of Production Cross-Sections & Spectroscopy
  - Measurements of “Weak Decays”
  - LF(U)V, CPV, Precision Measurements of Lifetime, Search/BR Measurement of Rare Decays, etc.
- Despite being a general purpose detector, competitive at flavor physics.
  - Large Statistics
  - Full Coverage → Phase Space Complements LHCb
  - Good Muon Performance
  - Often constrained by trigger bandwidth, however, constantly optimizing!

ATLAS detector

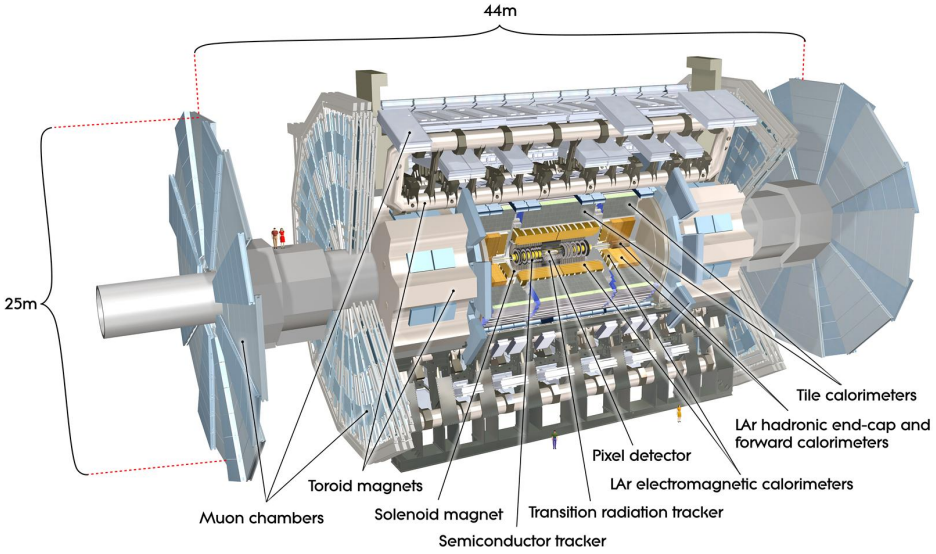

resolution is stable with luminosity!

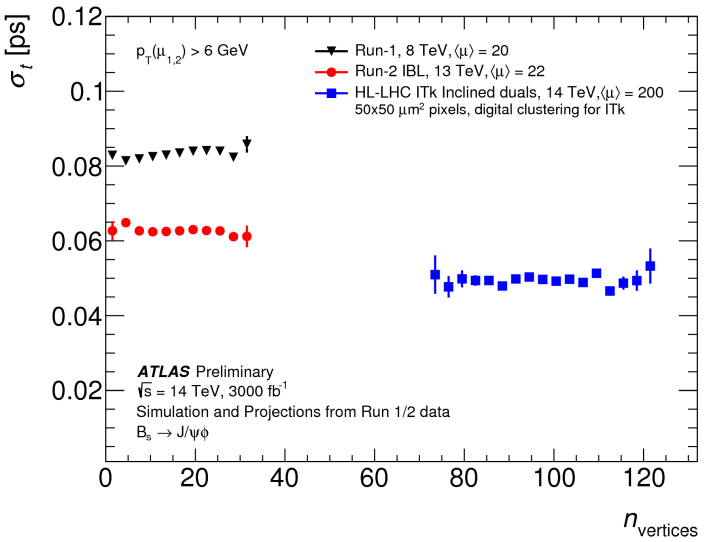

Time resolution of $B_s \rightarrow J/\psi\varphi$ for different numbers of reconstructed PV in the same bunch crossing PubNote

- Inner Detector: PIX, SCT and TRT, pT > 0.5 GeV, |η| < 2.5
  - Run2: new IBL 25% improvement of time resolution with respect to Run1.
  - Time, mass resolutions remain stable within increasing pileup in Run 2
- Muon Spectrometer: triggering (|η|< 2.4), precision tracking (|η|< 2.7)

arXiv:2412.15742

JHEP 07 (2025) 86.

https://doi.org/10.1007/JHEP07(2025)086

Differential cross-section measurements of $D^{\pm}$ And $D^{\pm}_{s}$ meson production in proton-proton collisions

$D^{\pm}$ and $D^{\pm}_{s}$: Context

- Measurements distinguish between promptly produced (hadronization of charm quarks from the primary hard scatter) and non-promptly produced (c produced through decays of b-hadrons).
- ALICE, CMS and LHCb have measurement from partial run-2 datasets.
- ATLAS has a measurement from run-1 although this is the first measurement production cross section of the D_s differentially.
- Compared with two theoretical models:
  - General-mass Variable-flavor-number (GM-VFNS)* - charm quark PDF evolves with massless evolution, heavy quark mass retained in the hard-scattering calculation.
  - Fixed-order next-to-leading-log (FONLL)** - heavy quark production x-section calculated in perturbative QCD, heavy flavor fragmentation is non-perturbative, and a decay function describes the heavy hadron decay into leptons.

*B.A. Kniehl et al. PRL 96 (2006) 012001; B.A. Kniehl et al., PRD 71 (2005) 014018; B.A. Kniehl et al., PRD 79 (2009) 094009; M. Benzke et al., JHEP 12 (2017) 021;
B.A. Kniehl et al., PRD 71 (2005) 094013.
**M. Cacciari et al., JHEP 05 (1998) 007; M. Cacciari et al., JHEP 10 (2012) 007.

$D^{\pm}$ and $D^{\pm}_s$: Method

- Require 2 muons with opposite charge, with $p_{1,T} > 6$ and $p_{2,T} > \{6 \text{ or } 11\}$, and each $|\eta| < 2.5$
- dimuon invariant mass consistent with ϕ-meson (inside a window of width that scales with $|\eta|$)
- The primary vertex is refit to remove the 3 candidate tracks.
- Background is suppressed by:
  - $L_{xy}/\sigma(L_{xy}) > 3$ and $|a_{xy}^0/\sigma_{axy0}| < 4$
  - Suppress combinatorial background through goodness of the SV fit
  - To match detector coverage and trigger acceptance, final candidate must have pT > 12 GeV and $|\eta| < 2.5$
  - In case of multiple candidates per event, the one with the best SV is selected.

$$L_{xy} = |\vec{L}_T| cos\theta_{xy}$$
$$a^0_{xy} = |\vec{L}_T| sin\theta_{xy}$$

$|\vec{L}_T|$ connects the SV and PV in the transverse plane.

θ_{xy} is the angle between $\vec{L}_T$ and the $\vec{p}_T$ of the μμπ candidate

- Reconstruction efficiency depends on prompt vs non-prompt, so constrain the non-prompt fraction by comparing data to lifetime templates from simulation (to constrain MC not measured officially).
- Divided 9 pt bin x 5 |η| bins, apply reconstructed efficiencies – derived from MC
- Unbinned maximum likelihood fit to the data, modeled with:
  - for signal: a Voigtian distribution (convolution of Breit-Wigner and gaussian)
  - for bkg (combinatorial): quadratic exponential

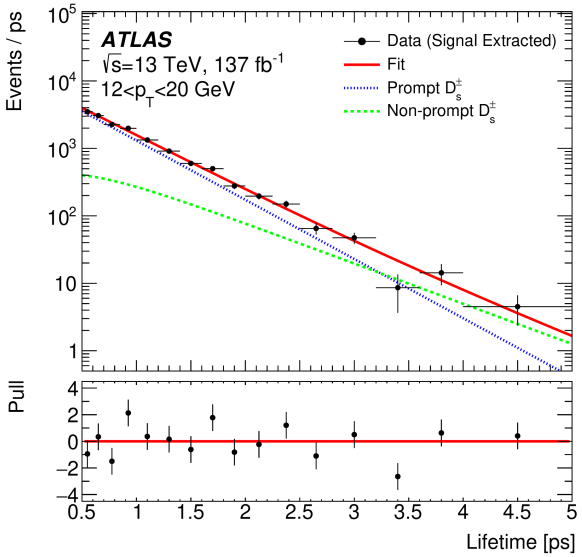

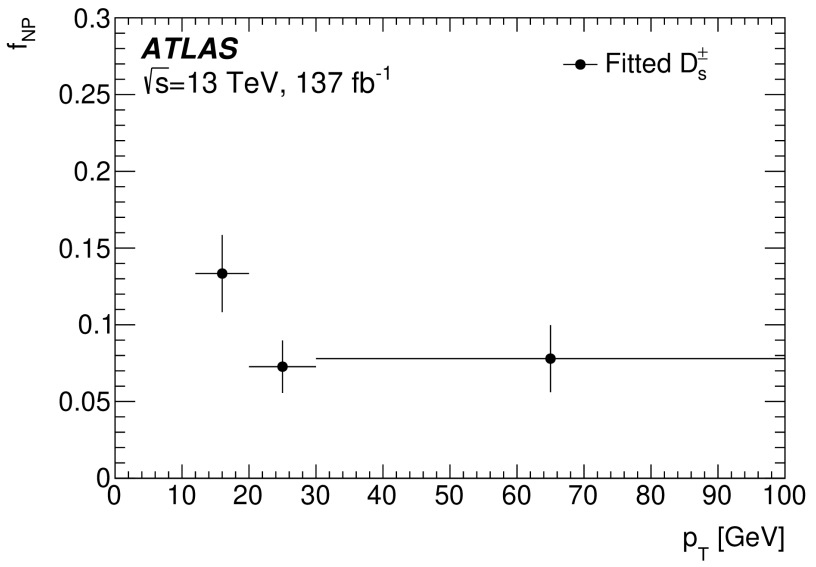

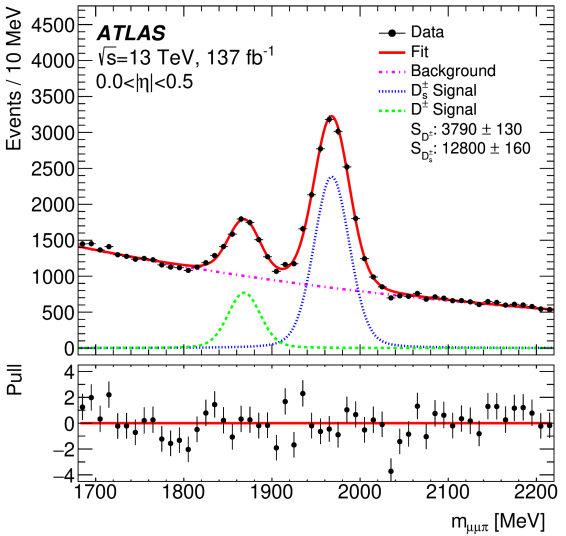

For $D^{\pm}$, good agreement with both models at low p_T. At higher pT, GM-FNS is higher; FONLL remains consistent with data.

For Ds, only GM-VFNS is available, and it predicts higher x-section throughout range, trending larger with pT.

Both models agree well with data in |η|.

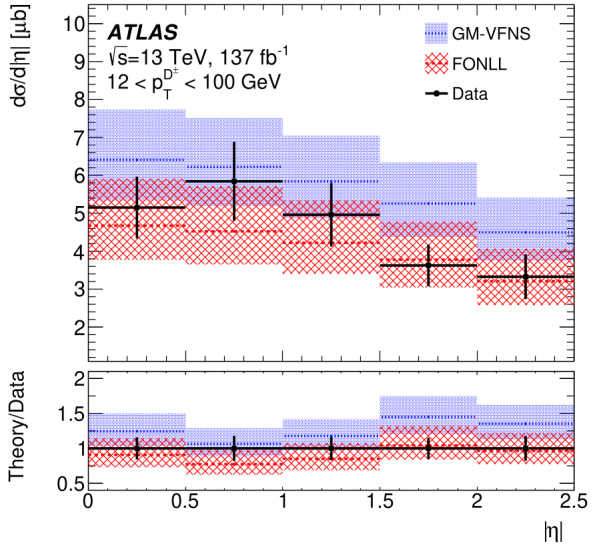

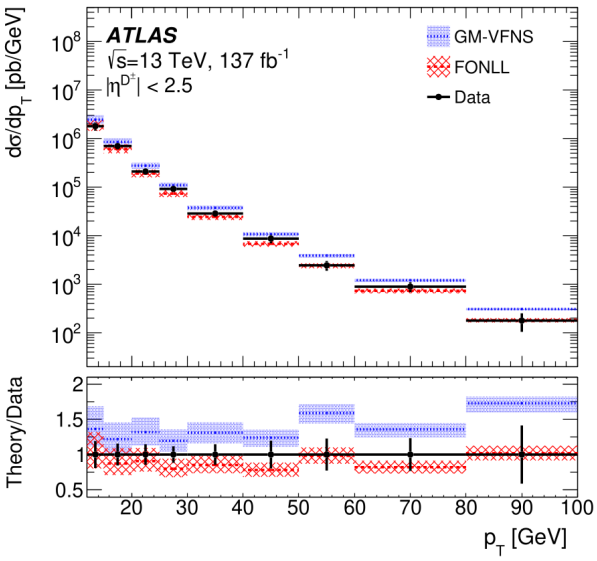

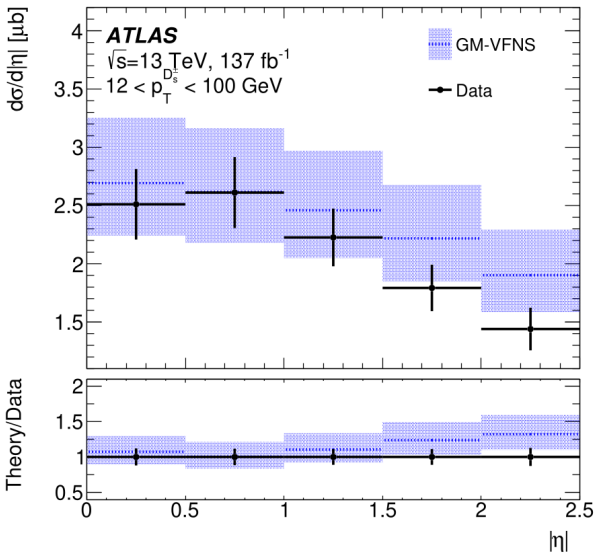

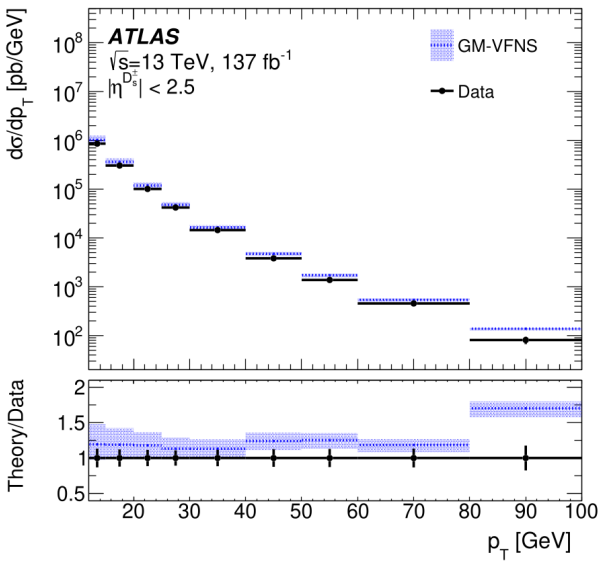

For the D_s, this is the first measurement in the differential cross section reported by ATLAS, and the first time such a measurement is reported up to pT ~100 GeV.

The D_s uncertainty of 12% at √s = 13 TeV improved relative to the 20% uncertainty at √s= 7 TeV.

The $D^{\pm}$ uncertainty of 14% at √s = 13 TeV is higher than the 11% uncertainty at √s = 7 TeV due to background uncertainty driven by low signal yield.

Data are mostly consistent with models within uncertainties, although the ratios predicted by GM-VFNS and FONLL are significantly different.

	$D^{\pm}$ inclusive fiducial cross-section [nb]		
	ATLAS	GM-VFNS	FONLL
	$\sigma \pm \delta_{\text{total}}$	$\sigma \pm \delta_{\text{theory}}$	$\sigma \pm \delta_{\text{theory}}$
$\sqrt{s} = 13$ TeV	$1\,690 \pm 270$	$2\,200^{+310}_{-290}$	$1\,480^{+230}_{-190}$
$\sqrt{s} = 7$ TeV	888 ± 97	980^{+120}_{-150}	620^{+100}_{-80}
Ratio (13 TeV/7 TeV)	1.9 ± 0.4	2.24 ± 0.04	2.38 ± 0.01

	$D_s^{\pm}$ inclusive fiducial cross-section [nb]	
	ATLAS	GM-VFNS
	$\sigma \pm \delta_{\text{total}}$	$\sigma \pm \delta_{\text{theory}}$
$\sqrt{s} = 13$ TeV	810 ± 100	950^{+140}_{-130}
$\sqrt{s} = 7$ TeV	510 ± 100	470^{+56}_{-69}
Ratio (13 TeV/7 TeV)	1.6 ± 0.4	2.02 ± 0.05

arXiv:2411.09962

Accepted by EPJC

Precision measurement of the B^0 meson lifetime using $B^0 \to J/\psi K^{*0}$ decays

$B^0 \rightarrow J/\psi K^*$: Introduction

- ATLAS has an analysis of the $B_s \rightarrow$ J/ψ phi (Eur. Phys. J. C 81 (2021) 342). To help validate this we measure the $B_d \rightarrow$ J/ψ K* lifetime.
- Particle lifetime is a fundamental property of primary phenomenological importance. The b-hadron lifetimes can be computed in the heavy-quark expansion (HQE) framework.
- Models typically provide predictions in ratios of b-hadron lifetimes. Lifetime differences are largely attributable to corrections for Pauli interference and weak annihilation which are enhanced by a phase space factor. That factor includes a non-perturbative matrix of four-quark operators recently calculated using QCD sum rules formulated in HQET.

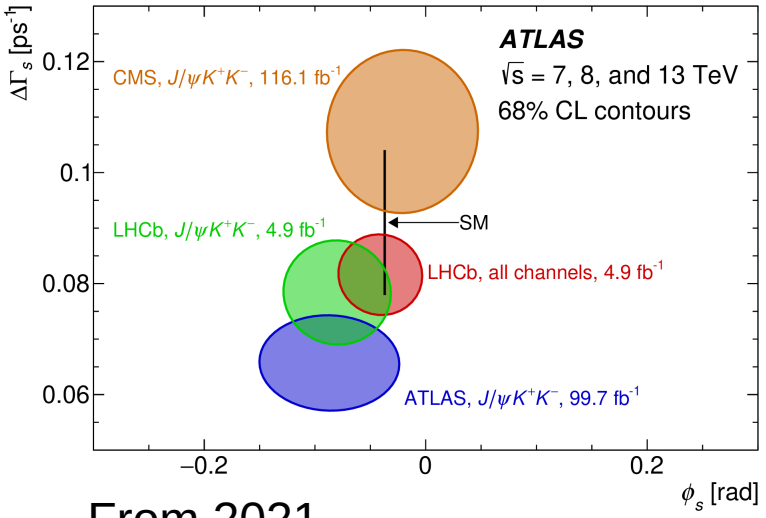

From 2021 (Eur. Phys. J. C 81 (2021) 342) Note CMS are publishing an updated analysis

Data-taking conditions for this analysis

- The measurement uses 2015-2018 pp collision data at sqrt(s) = 13 TeV.
- Triggers: J/ψ → μ+ μ− , the muon pT thresholds varying: 4 GeV, 6 GeV and 11 GeV.
  - Low pT thresholds were activated in the end of fills when the instantaneous luminosity decreases.
- For events accepted for this analysis, an average number of pp interactions per bunch crossing (pile-up) was 31.
- No displaced J/ψ vertex cuts applied. Trigger tracking: transverse parameter d0 < 10mm on all tracks.

B → J/ψK*0 candidates

- At least one J/ψ → μ+ μ− with χ^2 ndof < 10; within mass window retaining 99.7% J/ψ candidates.
- K* : Out of two hypothesis $K^+ \pi^-$ / $K^- \pi^+$ the one closer to K^* PDG mass selected.
- J/ψ and K* - fitted to a common vertex, constrained by fixing di-muon mass to J/ψ PDG. Only χ2 /ndof <3 retained.
- 10% events have multiple J/ψK* candidates (in average 2.1); the one with smallest χ^2 /ndof selected.

Mass PDFs of Signal and Background

- Signal mass is modelled with a Johnson distribution
- Background has two components:
  - 1. prompt - J/ψ produced in pp → J/ψX, combined with random K* .
  - 2. combinatorial - J/ψ from any b-hadron decay combined with random K*. They are modelled by sum of linear and sigmoid functions:

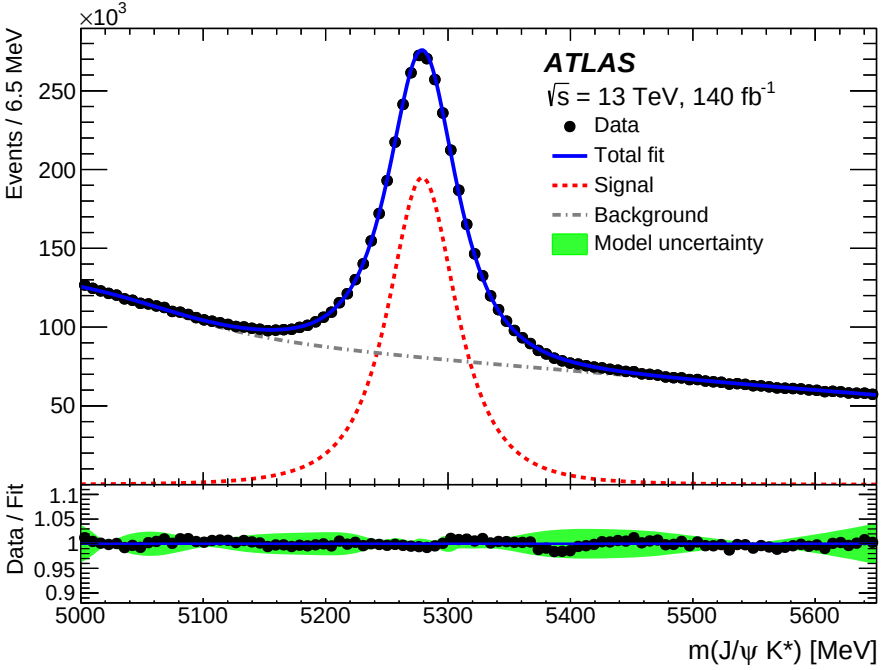

$$\mathcal{M}_{\text{bkg}}(m_i) = f_{\text{poly}}(1 + p_0 \cdot m_i) + (1 - f_{\text{poly}})\left(1 - \frac{s(m_i - m_0)}{\sqrt{1 + (s(m_i - m_0))^2}}\right)$$

$$\mathcal{M}_{\text{sig}}(m_i) = \frac{\delta}{\lambda\sqrt{2\pi}\sqrt{1 + \left(\frac{m_i - \mu}{\lambda}\right)^2}} \exp\left[-\frac{1}{2}\left(\gamma + \delta \sinh^{-1}\left(\frac{m_i - \mu}{\lambda}\right)\right)^2\right]$$

where μ, γ, δ and λ are free parameters of fit.

where f_{poly} relative size of the two components and m_0, s and p_0 are parameters of the fit

Proper-decay Time PDFs of Signal and Background

- Signal PDF: exponential function convolved by Resolution function R.

$$P_{\mathrm{sig}}(t_i|\sigma_{t_i}, p_{\mathrm{T}_i}) = E(t', \tau_{B^0}) \otimes R(t' - t_i, \sigma_{t_i})$$

$E(t', \tau_{B^0}) = (1/\tau_{B^0}) \exp(-t'/\tau_{B^0})$ for $t' \geq 0$, with τ_{B^0} - the fitted B^0_d lifetime.

- Background PDF:

$$P_{\mathrm{bkg}}(t_i|\sigma_{t_i}, p_{\mathrm{T}_i}) = \left(f_{\mathrm{prompt}} \cdot \delta_{\mathrm{Dirac}}(t') + (1 - f_{\mathrm{prompt}}) \sum_{k=1}^{3} b_k \prod_{l=1}^{k-1} (1 - b_l) E(t', \tau_{\mathrm{bkg}_k}) \right) \otimes R(t' - t_i, \sigma_{t_i})$$

Dirac function δ_{Dirac}: direct background; 3 exponentials $E(t', \tau_{\mathrm{bkg}_k})$: components of combinatorial background; τ_{bkg_k}, and fractions: f_{prompt} and b_k are free parameters of fit.

Resolution function *R*: modelled as a sum of three Gaussian distributions with widths: $S^{(k)}\ \sigma_{\tau_i}$

$$R(t' - t_i, \sigma_{t_i}) = \sum_{k=1}^{3} f_{\mathrm{res}}^{(k)} \frac{1}{\sqrt{2\pi}\ S^{(k)}\ \sigma_{t_i}} \exp\left(\frac{-(t' - t_i)^2}{2(S^{(k)}\ \sigma_{t_i})^2} \right)$$

three $f_{res}^{(k)}$ fractions and scale factors $S^{(k)}$ are free parameters of fit, σ_{τ_i} is the per-candidate time error, extracted from data in the vertex fit of each $B^0 \to J/\psi K^{*0}$.

Conditional probability and efficiencies

- Per-candidate time errors $\sigma_{\tau i}$, extracted from data in the vertex fit of each B_d^0 are used in the Resolution function R for deconvolution of proper decay times.
- Trigger, offline reconstruction, event selections bias reconstructed proper-decay time distribution.
- Trigger and offline tracking impose $|d_0| < 10$ mm, for all four final-state tracks of $B^0 \rightarrow J/\psi K^{*0}$, resulting in inefficiency at large times.

$$\mathcal{T}_j(\tau_i, \sigma_{\tau_i}, p_{T_i}) = P_j(\tau_i, \sigma_{\tau_i}, p_{T_i}) \cdot C_j(\sigma_{\tau_i}, p_{T_i}),$$

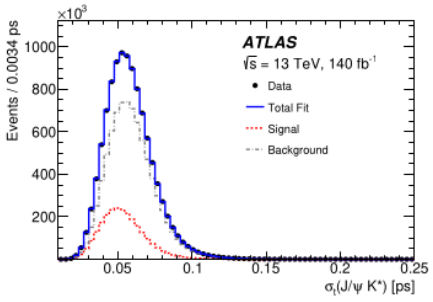

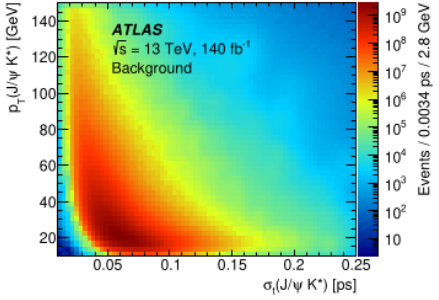

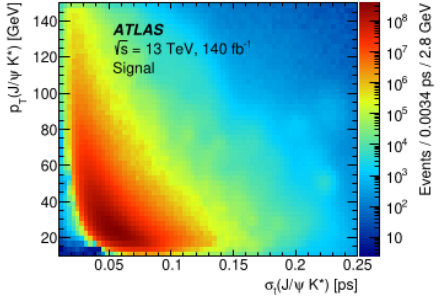

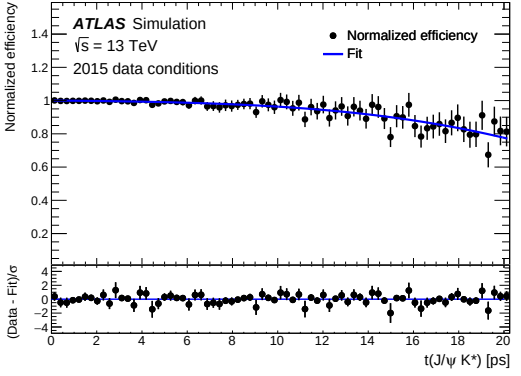

Systematic uncertainties

Source of uncertainty	Systematic uncertainty [ps]
ID alignment	0.00108
Choice of mass window	0.00104
Time efficiency	0.00130
Best-candidate selection	0.00041
Mass fit model	0.00152
Mass-time correlation	0.00229
Proper decay time fit model	0.00010
Conditional probability model	0.00070
Fit model test with pseudo-experiments	0.00002
Total	0.0035

Results

- The B^0 effective lifetime value measured with a total of 2 450 500 ± 2400 $B^0 \rightarrow J/\psi\ K^*$ signal events The measured effective lifetime is

$$\tau = 1.5053 \pm 0.0012\ (\text{stat.}) \pm 0.0035\ (\text{syst.})\ \text{ps}.$$

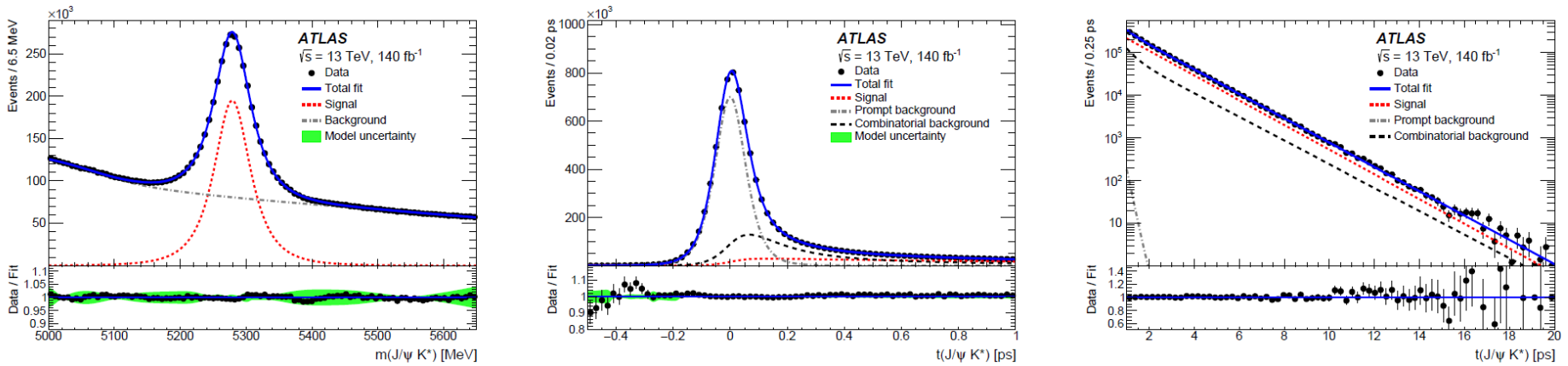

Mass fit projection (left). Proper decay time fit projections in two different ranges: (-0:5; 1:0) ps (Middle) and (1; 20) ps (Right). Solid blue line - total fit, dashed red line – signal.
The lower panels: ratio of data point to the fit value. The green band - the envelope of model variations included in the systematic uncertainty, the bars on the data points indicate statistical uncertainties. Plot-right - the model variation band too small to be visible.

Result Comparison

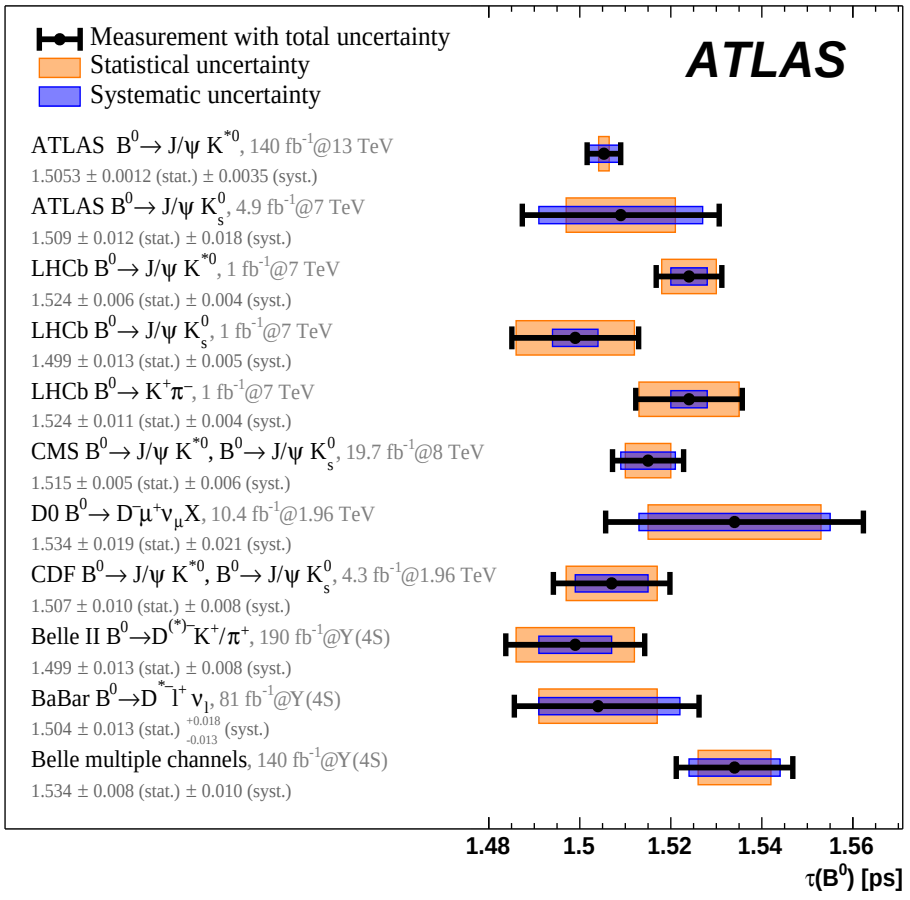

Results:

- $\tau_{B^0} = 1.5053 \pm 0.0012(stat.) \pm 0.0035(syst.)$ ps
- $\Gamma_d = 0.6639 \pm 0.0005(stat.) \pm 0.0016(syst) \pm 0.0038(ext.)$ ps^{-1}
- $\Gamma_d/\Gamma_s = 0.9905 \pm 0.0022(stat.) \pm 0.0036(syst.) \pm 0.0057(ext.)$

- Compatible with most other world measurements
- Reduced systematic uncertainty by factor 4.7 relative to previous (7 TeV, $B^0 \rightarrow J/\psi K_s{}^0$) ATLAS measurement
- Improvement due to data from the Insertable B-Layer, improved alignment, and increased statistics
- Γ_d is compatible with the HQE prediction* of $0.63^{+0.11}_{-0.07}$ ps^{-1}.
- Γ_d/Γ_s is compatible with predictions by HQE* (within 1.3σ) and lattice QCD** (within 0.4σ) and with the world average*** (within 1.3 σ)

Conclusions

- ATLAS has continues to make competitive measurements in Flavour Physics.
- Worldwide best measurement of B^0 lifetime.
- New measurement of the differential cross section of the D_S and $D^{\pm}$.
- For more BLS results check out our Twiki page

Backup Slides

Measurement of the production cross-section of J/ψ and ψ(2S) mesons

Measurement of the production cross-section of J/ψ and ψ(2S) mesons - Prompt

Eur. Phys. J. C 84 (2024) 169

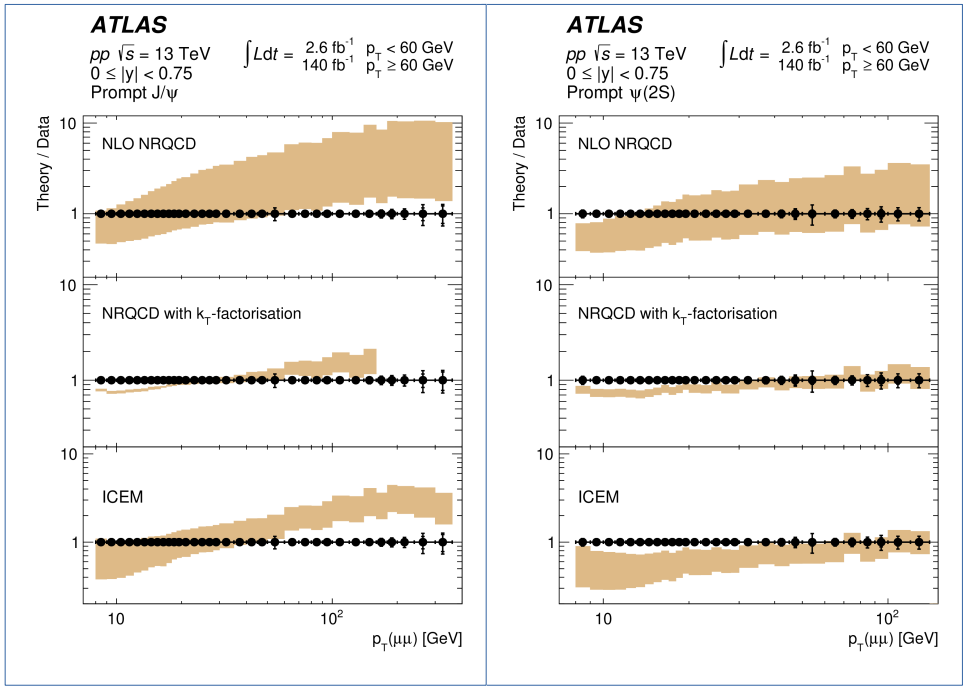

For NRQCD: Predictions and data largely overlap within theoretical uncertainties, which relate to renormalization, factorization, and NRQCD scales. Predictions overestimate data cross sections at high p_T.

For kT-factorization model: aims to improve the description by taking into account the transverse degrees of freedom of the initial gluons in the colliding protons. Uncertainties include only the renormalization scale. Prediction underestimates data at low p_T. High-p_T comparison is limited by availability of the p_T-dependent gluon PDF.

Improved Colour Evaporation Model (ICEM) assigns a fixed fraction of the $c\bar{c}$ and $b\bar{b}$ production cross section below the open charm threshold to individual charmonium states. Predictions use parameter values previously determined from LHCb 7 TeV data. Predicts harder pT spectra and underestimates the ψ(2S) cross section.

widest range of pT for J/ψ so far!

Measurement of the production cross-section of J/ψ and ψ(2S) mesons - Non-Prompt

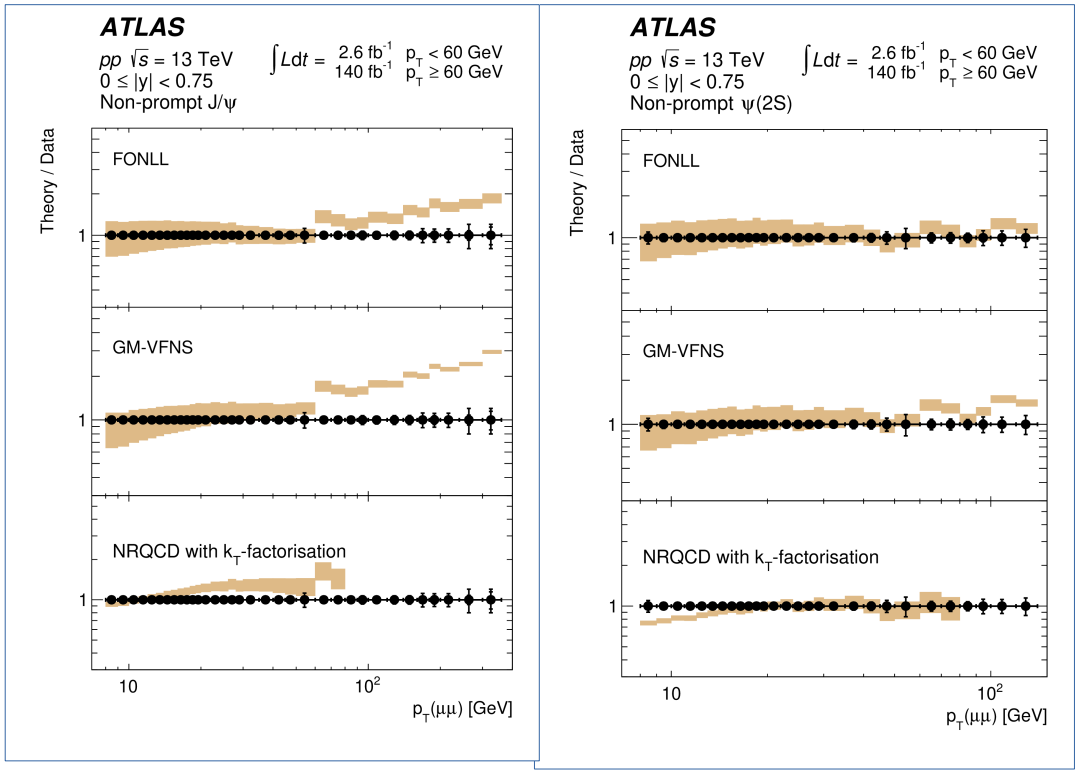

FONLL uncertainties cover renormalization scale and c-quark mass. Agreement at low p_T; prediction diverges at high p_T for J/ψ.

GM-VFNS uncertainties originate from renormalization scale dependence. Result similar to FONLL but with increased deviation at high p_T.

NRQCD with kT-factorization can be used to predict p_T distributions of vector charmonia through non-prompt production. Shapes are produced well but are limited by the available gluon PDF.

Systematic uncertainties: Mass-time correlation systematics

- Correlations between the invariant mass and the pseudo-proper decay time, and their potential impact on the fit results, are studied.
- No mass-time correlation in signal PDF proven by MC.
- For background the correlations are studied in data. First, applying the default time Background PDF Pbkg (t_i , σ_i , p_{Ti}) fit in each of the 6 mass sideband bins in data. Fractions fprompt and b1 , b2 determined in each bin were then fitted to extract their dependence on mass. The best description - achieved by linear functions.
- Based on this information, an alternative fit model, in which the background PDF term Pbkg (t_i, σ_i , p_{Ti}) is constructed with the parameters accounting for mass-dependence: